# Decoding Gender and Musical Expertise From Brain Responses to Music: A Comparison of Functional Connectivity Measures

Thesis submitted in partial fulfillment
of the requirements for the degree of

*Master of Science in*
***Electronics and Communication Engineering***
*by Research*

by

Arihant Jain
201431001
arihant.jain@research.iiit.ac.in

International Institute of Information Technology
Hyderabad - 500 032, INDIA
January 2024

International Institute of Information Technology
Hyderabad, India

# CERTIFICATE

It is certified that the work contained in this thesis, titled **"Decoding Gender and Musical Expertise From Brain Responses to Music: A Comparison of Functional Connectivity Measures"** by Arihant Jain, has been carried out under my supervision and is not submitted elsewhere for a degree.

_____ _____

Date Adviser: Dr. Vinoo Alluri

To Hope

# Acknowledgments

First and foremost, I extend my heartfelt gratitude to my thesis advisor, Dr. Vinoo Alluri, for her unwavering guidance and mentorship throughout this journey. Her insightful feedback, patience, and expertise have been invaluable in shaping this research and refining my understanding of the subject matter. Secondly, I want to thank Prof. Petri Toiviainen for helping out while ideating, writing the papers, and providing critical comments.

I am indebted to my family and friends for their constant love and belief in my abilities that I could complete this. I especially want to thank Arjit Srivastava for being my mentor, guiding me through this, and holding me accountable for not completing the tasks. Sakshi for her constant support, encouragement, and always lending a listening ear when needed. Lastly, Papa and Mummy for their unwavering love, sacrifices, and never-ending question, 'When are you finishing it?' that made this possible.

I am grateful to IIIT for providing access to the necessary resources and facilities that significantly contributed to completing this work.

Finally, I would like to thank myself for finishing this and not giving up whenever it felt like it couldn't be done.

# Abstract

Individual differences, encompassing a wide array of physical, cognitive, and emotional characteristics such as age, gender, personality, musical expertise, and empathy, play a pivotal role in shaping our interactions with the world around us. These differences, stable over time and across situations, not only influence our end goals but also the processes through which we perceive and interact with them. Recent research in neuroscience has brought to light that each individual possesses unique and fundamentally stable functional brain connections. These connections remain consistent, irrespective of the task at hand, suggesting that functional brain networks could potentially be employed as a measure of stable individual traits. Such an approach could revolutionize personalized medicine, offering tailored therapeutic interventions based on an individual's unique brain signature.

In the context of music, distinct patterns in functional brain networks related to individual differences become crucial. Music, as a continuous task, offers a naturalistic paradigm to explore these patterns. This study aims to bridge the gap in the existing literature by examining how brain responses to music may vary based on individual characteristics, such as gender and musical expertise. Furthermore, previous studies have predominantly focused on Pearson correlation, which captures linear relationships but may not encapsulate the full complexity of functional brain networks. Therefore, our study explores various functional connectivity (FC) measures. By comparing these measures, we aim to understand which ones are most suitable for a given study, ensuring that the chosen measures capture the intricacies of FC effectively.

The study utilized data from the "Tunteet" project, which involved multiple fMRI scans and behavioral tests. A total of 36 participants underwent fMRI scanning while listening to three distinct 8-minute-long musical pieces representing different musical styles. Their responses were analyzed using various temporal and spectral FC measures. The aim was to compare these FC measures to identify the one that captured the most variation associated with gender and musical expertise. Subsequently, a binary Support Vector Machine (SVM) was employed to classify distinct population groupings.

Our results align with previous research, suggesting that musical preferences can indeed be considered as a distinct personality trait. This was particularly evident in the differences in liking ratings specific to gender and musical expertise. We also found that Coherence, a spectral-domain FC measure, captured the maximum variation for musical stimuli. However, when classifying individuals based on gender and musical expertise, a composite measure, which combined all measures obtained by concatenation followed by a feature selection procedure, outperformed any single measure. This composite

measure consistently achieved better results, suggesting that each FC measure captures different aspects of the relationship between brain regions.

In summary, our research offers a fresh perspective on the interplay between musical preferences, gender, musical expertise, and brain responses. By leveraging diverse functional connectivity measures, we've shed light on the complexities of functional brain networks, paving the way for future research in this domain.

# Contents

# List of Figures

# List of Tables

*Chapter 1*

# Introduction

Individual differences include physical, cognitive, and emotional characteristics like age, gender, personality, musical expertise and training, and empathy. These differences are stable over time and across situations and influence not only our end goals but also the process of how we perceive them [1]. Recent research by Gratton et al. (2018) suggests that functional brain networks are dominated by common principles and unique features independent of the tasks and stable across task states. The study concluded that functional networks could be used to measure stable individual traits, which can be used in personalized medicine [2]. Therefore, exploring whether this unique brain signature can be leveraged to discern distinct patterns in fMRI data becomes crucial. Such an approach could facilitate the identification of specific individuals within a group, thereby enhancing our understanding of the variations that exist. Moreover, the potential to eliminate these unique brain signatures could lead to more reliable results in group-level studies.

Despite this approach's significance, more research needs to be focused on discerning distinct patterns in functional brain networks that relate to individual differences, particularly in a naturalistic paradigm where subjects are engaged in continuous tasks, such as listening to music. This study aims to address this gap by examining how brain responses to music may vary based on individual characteristics, such as gender and musical expertise.

While exploring distinct patterns in functional brain networks related to individual differences is crucial, it is also important to consider the limitations of certain measures used in this context. For example, the study by Gratton et al. (2018) focused on the Pearson correlation, which captures linear relationships but may not fully capture the complexity of functional brain networks. In contrast, the study by Mohanty et al. (2020) compared different functional connectivity measures and found that these measures capture different aspects of functional connectivity. Their findings suggest that FC patterns depend on the measure used to define them. Therefore, looking at various functional connectivity measures and comparing them is crucial to understanding which ones are most suitable for a given study.

## 1.1 Musical Preferences and Individual Differences

Past studies suggest that musical preferences reflect explicit characteristics such as age, gender, personality, musical expertise, and empathy [3, 4, 5, 6, 7]. For example, young people listen to music more often than middle-aged adults. They also listen to music in various contexts, whereas adults listen primarily in private contexts. Greenberg (2015) found in their study that people who are type E (bias towards empathizing) preferred music on the Mellow dimension (R&B/soul, adult contemporary, soft rock genres) compared to type S (bias towards systemizing) who preferred music on the Intense dimension (punk, heavy metal, and hard rock). Similarly, people who are open to new experiences tend to prefer music from the blues, jazz, classical, and folk genres, and people who are extraverted and agreeable tend to prefer music from the pop, soundtrack, religious, soul, funk, electronic, and dance genres [6].

In this thesis research, we focus on gender and musical expertise differences. We further discuss them in greater detail.

### 1.1.1 Gender

Several studies have explored differences due to gender in the brain that could underlie behavioral differences. Research has shown inherent structural differences between male and female brains. For instance, males have been found to have a higher proportion of white matter, while females have a higher proportion of gray matter which leads to larger brain volume in males and thicker cortex in females [8]. The corpus callosum, which connects the brain's two hemispheres, is larger and has more microstructural integrity in females [9]. The hippocampus, which is involved in memory, is larger in females, while the amygdala, which is involved in emotion processing, is larger in males [10]. These structural differences, which arise at a young age, translate to functional differences in adulthood. These differences have been observed in various cognitive tasks and sensory processing. Females show greater activation in the amygdala and hippocampus when processing emotional stimuli, which suggests that females are more attuned to emotional cues [11]. Studies have shown that male brains are better at intrahemispheric communication, while female brains are better at interhemispheric communication [12]. When listening to music, females show more bilateral activation in the auditory cortex than males, which is related to the structural differences in the corpus callosum [13].

Few behavioral studies have looked into gender as a critical factor in determining musical preferences [5, 3]. Evidence suggests that women prefer "softer" musical types like mainstream pop, while males prefer "harder" styles like rock [14]. This implies that such differences can manifest as differences in brain connectivity patterns during music listening. However, whether these gender differences can be predicted from brain responses to continuous music listening is yet to be shown.

### 1.1.2 Musical Expertise

Musical expertise is also known to cause structural and functional changes in the brain[15, 16, 7]. Musicians have been found to have increased gray matter volume in several brain areas, including the auditory cortex, motor regions, and areas involved in visuospatial processing [17]. Additionally, changes in white matter have been observed, which correlate with the onset and intensity of musical training [18]. Musicians also show structural differences in the cerebellum, which is involved in movement coordination – an essential aspect of playing an instrument [19].

Several studies have identified differences in functional connectivity due to musical expertise during continuous music listening [7, 20, 21]. Musicians exhibit enhanced auditory processing and are more sensitive to various elements of music such as pitch, timbre, and rhythm [22, 7]. Musical expertise has been associated with differences in functional connectivity during continuous music listening [20, 7]. This refers to the synchronization of neural activity between different brain regions, indicating that they are functioning in an integrated manner.

The structural and functional changes associated with musical expertise influences musical preferences. Gold et al. (2013) investigate how individual differences, including musical training, affect the ability to learn from pleasurable music, suggesting that musical training can influence musical preferences. To date, only one study by Saari et al. (2018) demonstrated the possibility of classifying individuals into musicians and non-musicians based on neural activations during naturalistic music listening. The study computed different low-level (timbre) and high-level (rhythm and tonality) musical features, representing different aspects of music perception from the acoustic signals. These features and the parcellated fMRI time series were then used to classify individuals into musicians and non-musicians. However, their approach did not focus on functional brain connections or how brain regions functioned in an integrated manner.

## 1.2 Introduction to Neuroimaging

Neuroimaging uses quantitative techniques to study the structure and function of the central nervous system (CNS), developed as an objective way of scientifically studying the healthy human brain in a non-invasive manner. It is being increasingly used for studies of brain disease and psychiatric illness. Neuroimaging technology provides accurate spatial (Structural) and temporal (Functional) characterization of cortical and subcortical regions and their activity. Structural Imaging is used to quantify brain structure. It is a modality that provides critical brain measurements such as cortical thickness, gray matter volume, and surface area. Functional Imaging is used to study brain function, using techniques like Electroencephalography (EEG), Positron Emission Tomography (PET), and Magnetic Resonance Imaging (MRI). MRI is the most modern and widely used of the three techniques. Although MRI is a new addition to functional imaging procedures, structural MRI has long been a standard method for diagnosing brain injuries and other associated disorders. Functional MRI (fMRI) came into existence

when BOLD (blood oxygen level-dependent) signals were initially proposed by Seiji Ogawa [23] in 1990.

In our research, we will mainly focus on fMRI as a neuroimaging technique to understand the dynamic functioning of the human brain.

### 1.2.1 Functional Magnetic Resonance Imaging (fMRI)

fMRI is a non-invasive brain imaging technique that indirectly measures brain function by measuring the hemodynamic response (changes in blood flow) resulting from neural activity. The main idea behind this is that of coupling between neural activation and blood flow, i.e., increased neural activity in some brain areas is linked to increased blood flow to those regions. fMRI tracks changes in blood flow by measuring the concentrations of oxyhemoglobin (Hb) and deoxyhemoglobin (dHb). Hemoglobin is an essential protein complex in the blood responsible for transporting oxygen to tissues on demand. Oxyhemoglobin refers to hemoglobin when it is attached to an oxygen molecule, and deoxyhemoglobin is hemoglobin without the attached oxygen molecule. When neurons in specific regions get activated, there is an increased demand for oxygenation, which is fulfilled by an increase in the local cerebral blood flow, replacing deoxygenated blood containing dHb with oxygenated blood containing Hb. Hb and dHb differ in their magnetic properties, with the former being diamagnetic and the latter being paramagnetic. Under the influence of the fMRI-induced magnetic field, dHb is attracted to the external field, thereby distorting it. This distortion, termed as Blood Oxygen Level Dependent (BOLD) signal, is picked up by the MRI scanner [24]. The MRI apparatus scans the BOLD response in slices, which are then quantized into three-dimensional homogenous units known as "voxels." The resolution of these voxels depends on the magnetic strength of the MRI apparatus, with 2mm being a popular resolution in neuroimaging studies. Each voxel has an associated time series capturing the temporal changes in the BOLD response of the region covered by that voxel.

fMRI data can be used to perform several analyses like functional connectivity analysis, graph theory-based brain network analysis, ROI-based analysis, seed-based analysis, and network-based analysis.

### 1.2.2 Traditional Task-based and Resting-state Paradigm

Traditional fMRI analysis tried identifying brain voxels with significant activations correlated with the presented stimulus or activity. These activations can be monitored by looking for variations in the BOLD response caused by changes in local cerebral blood flow. It is therefore critical to construct fMRI trials so that variations in the BOLD response reflect changes in the phenomenon under investigation rather than being caused by random noise or other secondary effects. As a result, most experimental designs predominantly employ a controlled paradigm with block and event-related designs. The primary notion in these situations is to divide the experimental condition/stimuli into intervals or blocks and then calculate the differential activity between the blocks and the resting/baseline condition. For example, in

an fMRI experiment designed to discover the neural basis of motor skill in guitarists, the BOLD response would be compared between the *Task*, in which participants move their fingers in a predetermined coordinated manner, and the *Baseline*, in which participants do not move their fingers. Such a paradigm excels at a segregated analysis, where various local regions specialized in processing the task in question are identified. This segregation allows for more straightforward interpretability of results as most other variations are controlled for, making this the most popular approach in neuroscience studies. However, this segregated approach combined with the controlled setting fails to identify large-scale networks that span the whole brain.

Resting-state fMRI (rs-fMRI) has been developed as an alternative to task-based fMRI, mapping brain processes by examining brain signals during rest. This method was first demonstrated in 1995 when it was shown that brain activations in the resting state could have similar brain region correlations as activations in the task state [25]. rs-fMRI examines the brain in a resting or task-negative state rather than the BOLD contrast between a task and a baseline (where participants do not perform explicit tasks). This design is based on a knowledge of intrinsic brain activity, meaning that differences in the BOLD response persist even when no external tasks are present. Researchers have explored functional connectivity patterns and the presence of large-scale networks in the brain using these rs-fMRI signals, which have very low amplitude variations and are often continuous, resting mostly within the 0.01 to 0.1 Hz range [26].

Past studies have used rs-fMRI data to classify schizophrenia, bipolar and healthy subjects based on their functional connectivity features [27, 28].

### 1.2.3 Naturalistic Task-based Paradigm

It was an intuitive shift toward a naturalistic task-based paradigm, given the shortcomings of traditional paradigms. In this paradigm, participants are presented with real-world (generally longer duration) stimuli such as movies or music without asking them to perform other tasks. The fMRI data from this paradigm tends to be continuous and very similar to the kind gathered in rs-fMRI experiments, presenting different challenges in its analysis compared to more traditional experiment designs.

Data from the block/event-related experiments assume that "the brain processes the various tasks/ events in isolation and that these independent processing events are characterized by a short, stereotyped burst of activity" [29]. This controlled paradigm lacks ecological validity since there is a vast difference between laboratory stimuli and most real-world stimuli. According to Zaki and Ochsner [30, 31], real-world information differs from lab stimuli in that it is generally multimodal, dynamic (involving information presented both serially and parallelly), and contextually embedded. Studies using visual stimuli have also found differences between brain responses in controlled and real-world settings [32], with real-world stimuli eliciting more widespread activations across various non-visual regions such as the motor cortex, which were absent in experiments performed in controlled settings. These differences become more pronounced when higher-order cognitive functions such as empathy or per-

sonality are examined due to the integrative nature of these processes [30]. These assumptions become invalid under the naturalistic setting.

Moreover, these uni-variate analysis techniques fail to capture the intrinsic connectivity patterns in the human brain accurately. This has led researchers to look into various multi-variate analysis techniques such as functional connectivity. In the analysis of neuroimaging time series, functional connectivity is defined as the statistical dependencies among spatially remote neurophysiologic events. It provides a simple characterization of functional interactions. It is further discussed in the next section.

## 1.3 Introduction to Functional Connectivity

Functional connectivity (FC) refers to the statistical dependencies among spatially remote neurophysiological events, providing a simple characterization of functional interactions [33]. The human brain is composed of functionally connected, spatially distributed areas that constantly exchange information among themselves. These connections between brain areas, known as brain networks, are the focus of functional connectivity studies. FC is the temporal dependence of the brain's physically dissociated neural activity patterns. Measurement of the coactivation level of fMRI time-series data between various brain regions has become a popular method for many studies to explore functional connectivity in recent years [34].

### 1.3.1 Why use different FC measures?

Conventionally, FC is defined by comparing the similarities between brain signals from two separate brain regions. Signals from two physically distinct brain regions may look associated under a conventional idea of similarity like Pearson's correlation, indicating that the regions are functionally connected in the brain [35, 36, 37]. A strong correlation between two regions does not necessarily guarantee a functional connection of the underlying neurons. Similarly, a low correlation value does not imply they have no dependence. It means that there is no linear relationship between them.

Although the ideas of similarity and dissimilarity seem straightforward, mathematical formulations show otherwise. Statistical relationships between two signals can develop in a variety of ways. It is possible that two distinct similarity measurements do not compare similarity in the same manner. A similarity and dissimilarity measure may not have a clear, straight inverse connection. Therefore, we need other measures which capture different aspects of statistical dependence between BOLD signals such as time-, frequency- and wavelet-domain information and linear, non-linear dependencies. These measures were then compared across various stimuli to examine the consistency of information offered by the FC measures and their utility in determining individual differences.

## 1.4 Thesis Objectives

- Explore whether unique functional brain networks can be used to identify individuals based on differences such as gender and musical expertise.
- Measure participants' fMRI responses while they are engaged in a continuous task like listening to music.
- Investigate different FC measures beyond the traditional Pearson's Correlation and understand how they capture interactions between different brain regions.
- Compare the effectiveness of different FC measures in classifying distinct population groups such as males-females, musicians-nonmusicians, and combined population groups.

## 1.5 Thesis Overview

The thesis is divided into a total of 5 chapters. Chapter 2 provides the details regarding the dataset we used in our study. In Section 2.1, we provide the participants' demographics of the fMRI music listening experiment and discuss the musical stimuli. Section 2.2 describe the steps followed in acquiring fMRI data and its pre-processing.

Chapter 3 describes the various methods and tools used to analyze the data. Section 3.2 describes in detail the different types of Functional Connectivity (FC) measures used in the study. In Section 3.4, we describe the supervised machine learning-based classification, feature selection, and feature importance used in our study.

In Chapter 4, we discuss how different FC measures are compared to one another and what information each of them captures. In Section 4.3 we provide and discuss the results and outcome of our study's various classification, feature selection, and feature importance approaches.

We finally conclude, discuss the limitations of our study, and discuss potential future work in Chapter 5.

*Chapter 2*

# Data Acquisition - Principles and Methods

The dataset used is part of a broader "Tunteet" project involving multiple fMRI scans and behavioral tests. This project was initiated and coordinated by Dr. Elvira Brattico and was approved by the Coordinating Ethics Committee of the hospital district of Helsinki and Uusimaa, Finland. The dataset consists of 77 participants with no prior neurological or psychological disorders who listen to music in a naturalistic paradigm while undergoing fMRI scanning. The participants were screened for inclusion before admission to the experiment (no ferromagnetic material in their body; no tattoo or recent permanent coloring; no pregnancy or breastfeeding; no chronic pharmacological medication; no claustrophobia). This dataset has been selected as it is a well-established dataset and has been previously used in multiple studies [20, 7, 38, 39, 40].

## 2.1 Participants and Musical Stimuli

### 2.1.1 Musical Stimuli

We used three western instrumental musical pieces from different genres of music. Each piece was about 8 minutes long. We did not choose lyrical music pieces to avoid the confounding effects of semantics. The music pieces were presented to the participants through MR-compatible in-ear headphones. After the fMRI scanning, the participants were asked to rate their liking for each piece and their familiarity with them on a 5-point Likert scale. The three pieces are as follows:

1. Astor Piazzolla's Adios Nonino (Genre: Tango Nuevo, further referred to as *Piazzolla*)

2. Igor Stravinsky's First Three Dances of the Rite of Spring (Genre: Modern Classical, further referred to as *Stravinsky*)

3. DreamTheater's Stream of Consciousness (Genre: Progressive Rock, further referred to as *DreamTheater*)

### 2.1.2 77 Participants, 1 Stimulus

Seventy-Seven participants' fMRI responses were measured while listening to Astor Piazzolla's Adios Nonino. Participants had no record of neurological or psychological disorders. The pool consisted of 26 musically trained and 51 untrained participants. Table 2.1 shows the demographics. Those labeled as musicians were required to have had at least five years of training and earned a degree in music or earned money for playing. The musicians were homogeneous in the time spent on active instrument playing and the duration of their musical training.

| **Groups** | **Musicians** | **Non-Musicians** |
|---|---|---|
| **N** | 26 | 51 |
| **Age** | $29.03 \pm 8.1$ | $29.84 \pm 9.34$ |
| **Gender** | 12F | 31F |
| **Hand** | 25R | 47R |
| **Active Listening (hrs/week)** | $10 \pm 9$ | $5 \pm 5$ |
| **Passive Listening (hrs/week)** | $14 \pm 11$ | $13 \pm 11$ |
| **Instruments** | Keyboard: 9<br>String: 9<br>Wind: 3<br>Percussion: 2<br>Mixed: 3 | - |
| **Instrument Starting Age** | $7.96 \pm 4.81$ | - |
| **Instrument Playing (years)** | $19.5 \pm 7.79$ | - |
| **Instrument Practising (hrs/week)** | $15.02 \pm 11.89$ | - |
| **Musical Training (years)** | $16.03 \pm 7.58$ | - |

Table 2.1: 77 Participants' Demographic Information.

### 2.1.3 36 Participants, 3 Stimuli

Eighteen musicians and eighteen non-musicians were then selected (based on the availability of behavioral measures) to form a pool of thirty-six participants. These participants' fMRI responses were measured for all three musical pieces. The three pieces were presented to the participants in a counterbalanced order. Both groups of participants were comparable in gender, age, cognitive measures

(WAIS-WMS III Scores of Processing Speed and Working Memory Index), and socioeconomic status (according to Hollingshead's Four-Factor Index). Table 2.2 shows the demographics for 36 participants.

| **Groups** | **Musicians** | **Non-Musicians** |
|---|---|---|
| **N** | 18 | 18 |
| **Age** | 28.2 $\pm$ 7.8 | 29.2 $\pm$ 10.7 |
| **Gender** | 9F | 10F |
| **Hand** | 18R | 17R |
| **Socio-Economic Status** | 43.6 | 35.4 |
| **WAIS-III Processing Speed Index** | 116.3 | 115.7 |
| **Active Listening (hrs/week)** | 7.5 $\pm$ 5.8 | 5.3 $\pm$ 4.8 |
| **Passive Listening (hrs/week)** | 10.6 $\pm$ 7.5 | 7.1 $\pm$ 3.9 |
| **Instruments** | Keyboard: 8<br>String: 6<br>Wind: 2 | - |
| **Instrument Starting Age** | 8.6 $\pm$ 5.5 | - |
| **Instrument Playing (years)** | 21.2 $\pm$ 7.8 | - |
| **Instrument Practising (hrs/week)** | 16.6 $\pm$ 11 | - |
| **Musical Training (years)** | 16 $\pm$ 5.7 | - |
| **Style** | Classical: 12<br>Jazz: 5<br>Pop-Rock: 1 | - |

Table 2.2: 36 Participants' Demographic Information.

## 2.2 fMRI Data Acquisition and Pre-Processing

The fMRI readings of the participants were acquired while they listened to the musical stimulus. During the scanning, participants were instructed to open their eyes and fix their gaze on their screen. The only task they had was to listen attentively to the music delivered through high-quality MR-compatible insert earphones. The music was played at a comfortable, audible volume. A 3T MAGNETOM Skyra whole-body scanner (Siemens Healthcare, Erlangen, Germany) and a standard 32-channel head-neck coil were used for the scanning conducted at the Advanced Magnetic Imaging (AMI) Centre (Aalto

University, Espoo, Finland). Thirty-three oblique slices (FoV = 192 x 192 mm; 64 x 64 matrix; slice thickness = 4 mm, interslice skip = 0 mm; flip angle = 75 degrees; echo time = 32 ms; voxel size: 2 x 2 x 2 $mm^3$) were acquired every 2 sec, using a single-shot gradient echo-planar imaging (EPI) sequence, providing whole-brain coverage for each participant.

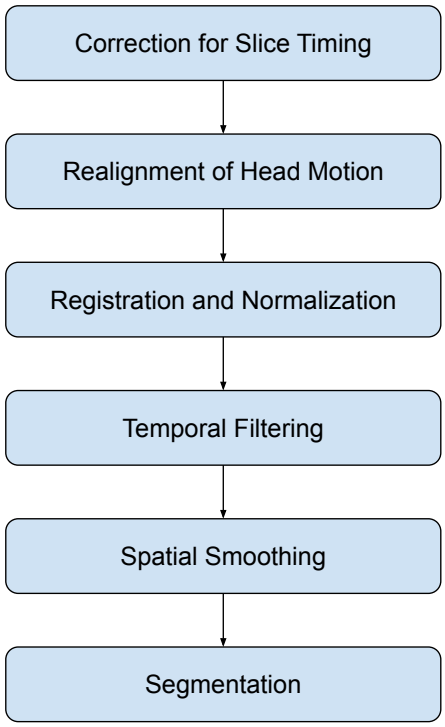


Figure 2.1: fMRI Data Preprocessing Steps

These fMRI images were preprocessed using SPM8 (Statistical Parametric Mapping), VBM5 (Voxel-Based Morphometry; Welcome Department of Imaging Neuroscience, London, UK), and custom scripts developed by us on the MATLAB platform. Preprocessing steps included:

1. **Correction for Slice Timing:** fMRI data is gathered via 2D MRI acquisition which involves acquiring data in slices. These slices take time to acquire and are either ascending (bottom to top) or descending (top to bottom) order. We model the data at each voxel, assuming that all of the slices were acquired simultaneously. For this assumption to be valid, the time series for each slice needs to be shifted back in time by the duration it took to acquire that slice. For studies with longer TRs (2s or longer), particularly in the dorsal areas of the brain, Sladky et al. (2011) demonstrated that slice-timing correction could lead to considerable gains in statistical power [41].

2. **Realignment of Head Motion:** Head movement causes many inaccuracies. To correct these unwanted movements, low-resolution images were realigned on six dimensions using rigid body

transformations (translation and rotation corrections were limited to 2 mm and 2 degrees, respectively).

3. **Registration and Normalization:** The images are registered to the corresponding high-resolution segmented T1-weighted structural images. Then normalized to the standard MNI 152 template (Montreal Neurological Institute) using 12-parameter affine transformations [42].

4. **Temporal Filtering:** fMRI data always has noise due to moderate drifting of the baseline signal over time. Removing this noise is called detrending of the data and is done using two methods: low pass and high pass filtering. Low pass filtering is used to remove signals with high peaks.

5. **Spatial Smoothing:** Spatial smoothing is done to eliminate the noise from the data. It reduces the spatial resolution but improves the signal-to-noise ratio (SNR). 8mm FWHM (full-width-at-half-maximum) Gaussian filter was used to perform spatial smoothing.

6. **Segmentation:** The image is then segmented into Grey Matter(GM), White Matter(WM), and Cerebrospinal Fluid(CSF).

The process resulted in $91 \times 109 \times 91$ voxels for each time point, which, when linearized, resulted in a matrix of 228453 voxels $\times$ 240 time-points for Piazzolla. Similarly, 228453 voxels $\times$ 230 time-points matrix for Stravinsky and 228453 voxels $\times$ 232 time-points matrices for DreamTheater. 4-time points were removed from each stimulus data for HRF delay.

*Chapter 3*

# Methods

## 3.1 Parcellation

The human brain is typically divided(or parcellated) into several anatomically and functionally distinct geographically contiguous regions to better comprehend the brain's functional architecture since neuroimaging data, particularly fMRI, has an unusually high spatial dimension. Accurate parcellations facilitate exact representations at multiple scales of whole-brain activity and efficiently compare results from different studies. Specifically, some functional connectivity (FC) based parcellation strategies divide a particular region of interest (ROI) into smaller, functionally specialized parcels by maximizing regions' functional homogeneity, which is typically measured with its functional coupling with other areas, or intra-area functional topographic organization [43].

Along with that, parcellating the brain data into smaller regions of interest also helps in ease of computation as a voxel size of $2 \times 2 \times 2$ mm results in a data dimension of $91 \times 109 \times 91$ at every time-point. Various diverse approaches have thus led to a variety of parcellation schemes, known as atlases, that provide a mapping of brain voxels to regions of interest. The atlas used in our study is the Willard Functional Atlas [**?**].

### 3.1.1 Willard Functional Atlas

Structure-based parcellations such as the AAL (Automated Anatomical Labeling) often comprise multiple, functionally independent regions. These independent regions have proven inferior to functionally defined regions in the classification of cognitive states [37] and in temporal and spatial clustering of brain regions [44]. Thus, we used a cortex-wide parcellation based on functional connectivity. More precisely, the Willard functional atlas, which consists of 499 functional ROIs (fROIs), generated by Bernard Ng [45] and derived from the 90 fROIs originally generated by William Shirer [37]. These 499 fROIs are further divided into three groups as per their overlap with the 90 fROIs atlas: a) 357 fROIs which have no significant overlap, b) 141 fROIs that significantly overlap, and c) 1 fROI which has modest overlap. For our analysis, we use 141 fROIs. To convert voxel data into 141 fROIs, the average

time series values across all the voxels within each region are calculated. This results in a time series of 141 fROIs × t time-points for every dataset participant.

## 3.2 Functional Connectivity Measures

We use various temporal, spectral and graph based measures to capture different statistical dependence aspects between two BOLD signals. These measures capture time-, frequency- and wavelet-domain information, linear and non-linear dependencies, and similarity and dissimilarity measures. These measures were then compared across various stimuli to examine the consistency of information offered by the FC measures and their utility in determining individual differences.

We use eight temporal-based, two spectral-based, and one graph-based measure. For each FC measure, we obtain a symmetrical functional connectivity matrix of size 141 x 141 for each stimulus for each individual. Each entry in the matrix represents FC between the corresponding pair of brain regions. All the FC analyses were performed using MATLAB.

Variables $x$ and $y$ would represent time series from any pairs of distinct regions with each $x,\ y\ \epsilon\ \mathbb{R}^t$. Pairwise FC, measuring the statistical dependence between all possible pairs in a given network would yield a matrix of size n × n. This would generate a symmetric matrix and can be reduced to n(n-1) unique coefficients(from either the upper or lower triangle of the matrix). The following defines and characterizes each identified measure quantifying FC, a summary of which is presented in Supplementary Table 2.

### 3.2.1 Temporal-Based

1. **Cityblock distance**: Cityblock (Manhattan) distance is a distance metric between two points in a N dimensional vector space. It is the sum of the lengths of the projections of the line segment between the points onto the coordinate axes. It is given by:

$$d_{cityblock} = \sum_{j=1}^{n} |x_{sj} - x_{ij}|, \tag{3.1}$$

where $x_s$ and $x_t$ are vectors from an $m$-by-$n$ matrix, which is treated as $m$ (1-by-$n$) row vectors $x_1, x_2, ..., x_m$. It was implemented using *pdist* function in Matlab with *distance=cityblock*.

Cityblock can decompose the contributions made by each variable of the signal in terms of the difference in their absolute values. As with euclidean, the measure cityblock is bounded below by 0, is not bounded above and scale-variant. Values closer to 0 are more desirable to claim lower dissimilarity between vectors. Unlike euclidean, which squares the difference in amplitudes and amplifies the deviation, the larger differences in cityblock are not amplified.

2. **Cross Correlation**: Cross-correlation is an extended version of Pearson's correlation as it calculates the linear correlation between all possible shifted versions of a signal relative to the other signal as follows:

   where $y_i^*$ represents the complex conjugate of $y_i$. Index $m$ is the displacement between the two signals and is called a lag or lead depending on whether it assumes a positive or negative value.

   Cross-corr ranges from -1 to 1, since it computes the correlation between displaces versions of two signals. A single similarity measure is produced by the correlation of two signals, whereas the cross-correlation of two signals produces a vector of similarity measures for any value of m. For a specific m, the vector's greatest value can be used as a feature in subsequent analysis. This could be helpful in identifying brain regions that might not be functionally connected simultaneously but become connected after a lag time. It was implemented using *xcorr* function in Matlab and maximum value across all possible shifts was used to measure FC.

3. **Dynamic Time Warping (DTW)**: DTW produces a distance metric between two input time series. Through non-linear warping of the time axis, it evaluates dissimilarity and aligns the signals. This metric is based on building a lattice and computing a local cost of similarity between each feasible pair of dimensions between two signals. The signals are positioned to have the greatest possible overall overlap based on this lattice (or minimum cost in the optimization framework). These are the steps involved:

   For two signals, $x$ and $y$, let $d_{ij}$ be the Euclidean distance between $i^{th}$-dimension of $x$ and $j^{th}$-dimension of $y$. All pairwise distances $d_{ij}$ are arranged into a lattice $C_{i,j}(x, y)$ of size $t * t$. Then $d_{dtw}$ searches through the lattice for a path parameterized by two sequences of the same length such that

   $$\sum C_{i,j}(x, y) \tag{3.2}$$

   is minimum. Without skipping any dimensions or repeating any signal dimensions, the chosen path aligns both signals. Here, all non-linear variations in the temporal domain are considered. Dynamic temporal warping is unbounded above and has a lower bound of 0 because it is a dissimilarity measure. Although the duration of the signals in the case of BOLD signals is the same, it is scale-variant and applies to the general scenario when signals are of different lengths in time. It was implemented using *dtw* function in Matlab with *metric=euclidean*.

4. **Earth Mover's Distance**: The Earth Mover's Distance (EMD) is a method to evaluate dissimilarity between two multi-dimensional distributions in some feature space where a distance measure between single features, which we call the ground distance is given. The EMD 'lifts' this distance from individual features to full distributions. Intuitively, given two distributions, one can be seen as a mass of earth properly spread in space, the other as a collection of holes in that same space. Then, the EMD measures the least amount of work needed to fill the holes with earth. Here, a unit of work corresponds to transporting a unit of earth by a unit of ground distance.

Treating $x$ and $y$ as probability distributions with:

$$x = \{(t_{x_1}, x_1), (t_{x_2}, x_2)...(t_{x_m}, x_m)\} \tag{3.3}$$

and

$$y = \{(t_{y_1}, y_1), (t_{y_2}, y_2)...(t_{y_n}, y_n)\} \tag{3.4}$$

where each $x_i$ is a cluster (=amplitude) of the signal $x$ at time-point $t_{x_i}$ and each $y_j$ is a cluster (=amplitude) of signal $y$ at time-point $t_{y_j}$. EMD can be computed with different values of $m$ and $n$, in case of BOLD signals, they can be considered to be the same for a given individual and determined by the scan length. Then the ground distance between clusters at $p_i$ and $q_j$ can be encoded in the matrix

$$D = [d_{i,j}] \tag{3.5}$$

with a flow between clusters at $p_i$ and $q_j$ represented by the matrix

$$F = [f_{i,j}] \tag{3.6}$$

The objective is to minimize the overall cost

$$min \sum_{i=1}^{m} \sum_{j=1}^{n} f_{i,j} d_{i,j} \tag{3.7}$$

while satisfying the following constraints:

$$f_{i,j} \geq 0 \, for \, 1 \leq i \leq m, 1 \leq j \leq n \tag{3.8}$$

$$\sum_{j=1}^{n} f_{i,j} \leq t_{x_i} \, for \, 1 \leq i \leq m \tag{3.9}$$

$$\sum_{i=1}^{m} f_{i,j} \leq t_{y_j} \, for \, 1 \leq j \leq n \tag{3.10}$$

$$\sum_{i=1}^{m} \sum_{j=1}^{n} f_{i,j} = min\{\sum_{i=1}^{m} t_{x_i}, \sum_{j=1}^{n} t_{y_j}\} \tag{3.11}$$

Earth mover's distance can then be defined as the amount of work needed to transform distribution $x$ to distribution $y$, normalized by the total flow

$$d_{emd}(x, y) = \frac{\sum_{i=1}^{m} \sum_{j=1}^{n} f_{i,j} d_{i,j}}{\sum_{i=1}^{m} \sum_{j=1}^{n} f_{i,j}} \tag{3.12}$$

Similar to DTW, EMD also considers non-linear interactions between signals and is scale-variant and applicable to general signals of unequal length. This measure is scale-bounded below by the distance between the centroids of the distributions or signals, and values closest to it represent more significant similarity. It was implemented using custom Matlab function *emd* which can be found here.

5. **Euclidean Distance**: Euclidean distance is a dissimilarity measure and it measures the geometric distance between two points. This can be computed by the following:

$$d^2_{euclidean} = (x_s - x_t)(x_s - x_t)', \tag{3.13}$$

where $x_s$ and $x_t$ are vectors from an $m$-by-$n$ matrix, which is treated as $m$ (1-by-$n$) row vectors $x_1, x_2, ..., x_m$. The difference terms serve as the measure of similarity. $d_{euclidean}$ is dependent on the magnitude of individual points of the vectors. While it is bounded below by 0 indicating low dissimilarity, there is no upper bound. However, it can be rescaled to range between 0 and 1 for interpretability. Euclidean distance is not invariant to the scale of the data. It must be applied once the data has been appropriately scaled. It was implemented using *pdist* function in Matlab with *distance=euclidean*.

6. **Mutual Information**: Mutual Information between two random variables measures non-linear relations between them. Besides, it indicates how much information can be obtained from a random variable by observing another random variable. The following formula shows the calculation of the mutual information for two discrete random variables $x$ and $y$ over the space $X$ x $Y$.

$$I(x;y) = \sum_{y \in Y} \sum_{x \in X} p(x,y) \cdot log \left( \frac{p(x,y)}{p(x)p(y)} \right), \tag{3.14}$$

where $p_x$ and $p_y$ are the marginal probability density functions and $p_xy$ the joint probability density function. Essentially, mutual information captures the information that is shared between $x$ and $y$, i.e., it measures how much knowing one of them reduces uncertainty about the other. It can assume non-negative values only. On one hand, if $I(x;y) = 0$, then knowledge of $x$ does not offer any knowledge of $y$ and vice-versa. On the other hand, if there exists a deterministic relationship between $x$ and $y$, then knowledge of $x$ is also shared with $y$ and vice-versa. In this case, $I(X;Y)$ is equivalent to the entropy of each $x$ as well as $y$ which represents the expected information stored by each random variable. It was implemented using custom Matlab function *mutualinfo* which can be found here.

7. **Pearson's Correlation**: Pearson's linear correlation coefficient is the most commonly used linear correlation coefficient. For column $X_a$ in matrix X and column $Y_b$ in matrix Y, having means $\bar{X}_a = \sum_{i=1}^{n}(X_{a,i})/n$, and $\bar{Y}_b = \sum_{j=1}^{n}(X_{b,j})/n$, Pearson's linear correlation coefficient $\rho(a,b)$ is defined as:

$$rho(a,b) = \frac{\sum_{i=1}^{n}(X_{a,i} - \bar{X}_a)(Y_{b,i} - \bar{Y}_b)}{\{\sum_{i=1}^{n}(X_{a,i} - \bar{X}_a)^2 \sum_{j=1}^{n}(Y_{b,j} - \bar{Y}_b)^2\}}, \tag{3.15}$$

where n is the length of each column. Values of the correlation coefficient can range from –1 to +1. A value of –1 indicates perfect negative correlation, while a value of +1 indicates perfect positive

correlation. A value of 0 indicates no correlation between the columns. It was implemented using *corr* function in Matlab with *Type=Pearson*.

8. **Spearman's Correlation**: Spearman's rho is equivalent to Pearson's Linear Correlation Coefficient applied to the rankings of the columns $X_a$ and $Y_b$. If all the ranks in each column are distinct, the equation simplifies to:

$$rho(a,b) = 1 - \frac{6\sum d^2}{n(n^2-1)}, \tag{3.16}$$

where d is the difference between the ranks of the two columns, and n is the length of each column. It essentially measures the strength of a monotonic relationship between two variables with the same scaling as the Pearson correlation. It was implemented using *corr* function in Matlab with *Type=Spearman*.

### 3.2.2 Spectral-Based

1. **Coherence**: The spectral coherence estimate is a function of frequency with values between 0 and 1. These values indicate how well $x$ corresponds to $y$ at each frequency. The magnitude-squared coherence is a function of the power spectral densities, $P_{xx}(f)$ and $P_{yy}(f)$, and the cross power spectral density, $P_{xy}(f)$, of x and y:

$$C_{xy}\left(f\right) = \frac{|P_{xy}(f)|^2}{P_{xx}(f)P_{yy}(f)} \tag{3.17}$$

Coherence value of 0 indicates no coherence between the signals and 1 indicates strong coherence between the signals. It can be considered to reflect the phase consistency between two signals at a given frequency. On one hand, a weaker coherence is the case when the signals share a random phase relationship and on the other hand, stronger coherence results when the phase relationship is almost constant between the signals. It was implemented using *mscohere* function in Matlab and maximum value across all possible frequencies was used to measure FC.

### 3.2.3 Spectro-Temporal-Based

1. **Wavelet Coherence**: Wavelet coherence captures similarity and quantifies how time signals from two sources are related in the time-frequency-domain. It is based on computing the cross-wavelet power which reveals the parts of the signals that share high common power. Wavelet coherence measures the coherence of the cross wavelet transform in time-frequency-domain and is given by:

$$WC(x,y) = \frac{|S(C_x^*(a,b)C_y(a,b))|^2}{S\left|C_x(a,b)\right|^2 \cdot S\left|C_y(a,b)\right|^2} \tag{3.18}$$

$C_x(a,b)$ and $C_y(a,b)$ denote the continuous wavelet transforms of $x$ and $y$ at scales $a$ and positions $b$. The superscript $^*$ is the complex conjugate and $S$ is a smoothing operator in time and scale. For real-valued time series, the wavelet coherence is real-valued if you use a real-valued analyzing wavelet, and complex-valued if you use a complex-valued analyzing wavelet. It was implemented using *wcoherence* function in Matlab and average value over the instances (top half only) showing highest similarity was used to measure FC.

2. **Instantaneous Phase Synchrony (IPS)**: IPS measures the phase similarities between signals at each timepoint. The phase refers to the angle of the signal when it is resonating between $0\ to\ 360$ degrees or $-\pi\ to\ \pi$ degrees. When two signals line up in phase their angular difference becomes zero. The angles can be calculated through the hilbert transform of the signal. Phase coherence can be quantified by subtracting the angular difference from 1. Let Y be a 2-dimensional matrix of size R × T (regions x time points). In the following equations, $z_{m_1}[t]$ and $z_{m_2}[t]$ are supposed to be the analytical representations of $y_{m_1}[t]$ and $y_{m_2}[t]$, that are the rows in Y:

$$\begin{aligned} z_{m_1}[t] &= y_{m_1}[t] + j\tilde{y}_{m_1}[t] = a_{m_1}[t]e^{j\phi_{m_1}[t]} \\ z_{m_1}[t] &= y_{m_1}[t] + j\tilde{y}_{m_1}[t] = a_{m_1}[t]e^{j\phi_{m_1}[t]} \end{aligned} \tag{3.19}$$

where $j = \sqrt{-1}$, $\tilde{y}$ is the Hilbert transform of y, $a_{m_1}[t]$ and $a_{m_2}[t]$ are the instantaneous amplitudes, and $\phi_{m_1}[t]$ and $\phi_{m_2}[t]$ are instantaneous phases of $y_{m_1}[t]$ and $y_{m_2}[t]$. The two signals $y_{m_1}[t]$ and $y_{m_2}[t]$ are said to be phase-locked of order 1:1 when:

$$abs(\phi_{m_1}[t] - \phi_{m_2}[t]) \approx 0 \tag{3.20}$$

We then quantified the instantaneous phase similarity between the two signal pairs $\phi_{m_1}[t]$ and $\phi_{m_2}[t]$ for all pairs of rows in the Z matrix as:

$$IPS_{m_1,m_2}[t] = abs(cos(\phi_{m_1}[t] - \phi_{m_2}[t])) \tag{3.21}$$

The IPS measure is a great way to compute moment-to-moment synchrony between two signals without arbitrarily deciding the window size as done in rolling window correlations. It was computed using custom Matlab scripts.

### 3.2.4 Graph-Based

For each participant, the functional connectivity matrix was generated by computing the Pearson correlation of the fMRI time series between every pair of voxels. This matrix was then made non-negative by incrementing each entry by 1. A power-iteration method was used to compute the first eigenvector for each participant's FC matrix. The result was a voxel-wise EC map for each participant (Refer to Eq. 1)(Fig. 1).

$$x_i = \frac{1}{\lambda} \sum_k FC_{k,i} x_k, \tag{3.22}$$

where, $x_i$ is centrality of $i$th node and $k$ denotes all voxels, $FC_{k,i}$ denotes the FC matrix value between nodes $k$ and $i$.

## 3.3 Sørensen–Dice Similarity Coefficient

The Sørensen–Dice coefficient is a statistic used to gauge the similarity of two samples. It was independently developed by the botanists Thorvald Sørensen[46] and Lee Raymond Dice[47] in 1948 and 1945, respectively. The similarity coefficient of two sets $A$ and $B$ can be expressed as:

$$dice(A, B) = \frac{2|A \cap B|}{|A| + |B|} \tag{3.23}$$

where $|X|$ and $|Y|$ are the cardinalities of the two sets (i.e., the number of elements in each set), and $\cap$ represents the intersection of two sets (elements common to both sets).

Each FC matrix was thresholded for our analysis to obtain a binary adjacency matrix. We used two thresholding methods: a) standard deviation higher and lower than the overall mean (mean $\pm$ c*std, where c = 1 and 2) [48], and b) average degree thresholding(S = 2.5 and S = 4) [49, 50, 51]. We observed similarities between different stimuli, groups, and FC measures.

- **Similarities across stimuli**: The similarity coefficient for each subject was calculated between all possible stimulus pairs(1 vs. 2, 2 vs. 3, and 1 vs. 3). These values were then pooled across all subjects, musicians, non-musicians, males and females to study group differences.
- **Similarities across groups**: Similarity coefficient was calculated for each stimulus between all possible subject pairs(males vs. females, musicians vs. non-musicians). The mean value for each stimulus was then calculated to compare different groups.
- **Similarities across FC measures**: FC matrices were averaged across all stimuli and subjects to generate mean FC matrices. Each element in the mean FC matrix was obtained by computing the mean of FC values in the cell of each of the corresponding individual matrices in the group. As mentioned earlier, binary adjacency matrices were subsequently obtained using threshold methods, and a similarity coefficient was calculated between all possible measure pairs.

Figure 3.1 shows the overview of our similarity pipeline.

## 3.4 Classification

Classification is a supervised machine learning technique used to identify the category of new observations based on training data. In classification, the algorithm learns from the given dataset and then

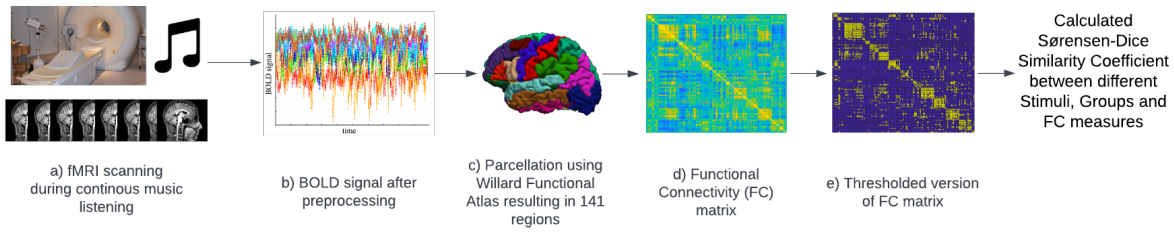


Figure 3.1: An overview of our similarity pipeline

classifies new(or unseen) observations into different classes or groups. The algorithm which implements the classification on a dataset is known as a classifier. There are two types of classification problems:

1. Binary Classification: It involves classifying data into only two classes.

2. Multi-Class Classification: It involves classifying data into three or more classes.

In neuroscience, machine learning is used for two purposes, encoding, and decoding. Encoding is the process of predicting or generating brain responses from external stimuli, while decoding is the method of understanding, analyzing, and deciphering neural responses in the brain. Our study pertains to decoding brain networks to identify the unique brain signatures in individuals. In order to identify gender and musical expertise from brain responses, we use a support vector machine (SVM) classifier.

For the training data, we utilized only the upper triangular matrix (of size $\frac{n(n-1)}{2}$, where n = 141 regions) due to the symmetry in the generated FC matrices. These vectors were then combined across subjects (feature vector size = 36 x $\frac{n(n-1)}{2}$) to form the training data. We used a leave-one-out strategy to maximize the size of the training dataset. We then performed feature selection on training data to reduce redundant features and noise. We used a Random Forest Regressor (RFR)[52, 53], an ensemble of individual decision trees, to reduce the feature set. It also provides feature importance in terms of weights that can be used to find crucial region-pair connectivity necessary to identify individuals. RFR was performed with the default number of trees in the forest (*n_estimators* = 100) as well as with variable numbers ranging from 10 to 1000, implemented using python's scikit-learn toolbox[54]. A meta-transformer (SelectFromModel) was followed, selecting features based on feature importance weights implemented using the same toolbox. Mean weight was used as the threshold value for feature selection.

### 3.4.1 Linear Support Vector Machine (SVM) Classifier

The SVM is a classifier that represents the training data as points in space separated into categories by a gap as wide as possible. New points are then added to space by predicting which category they fall into and which space they will belong to.

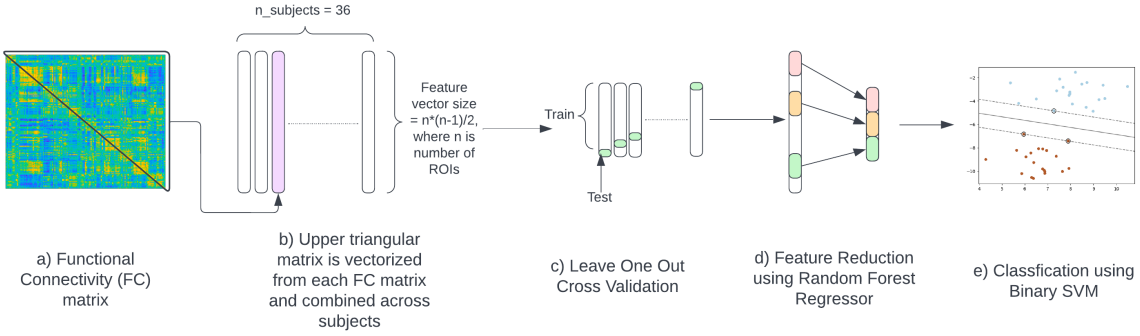


Figure 3.2: An overview of our classification pipeline

In the scikit-learn package, the Linear Support Vector Machine Classifier is implemented in the class LinearSVC, present in the sklearn.svm API package **??**. It is implemented in terms of liblinear, which provides it more flexibility in the choice of loss functions and penalties and makes it easier to scale to a large number of samples instead of just using the SVC class from the same package with the hyperparameter kernel='linear', which uses libsvm. As LinearSVC is inherently a binary classification model, the model uses a one-vs-rest scheme for multi-class classification support.

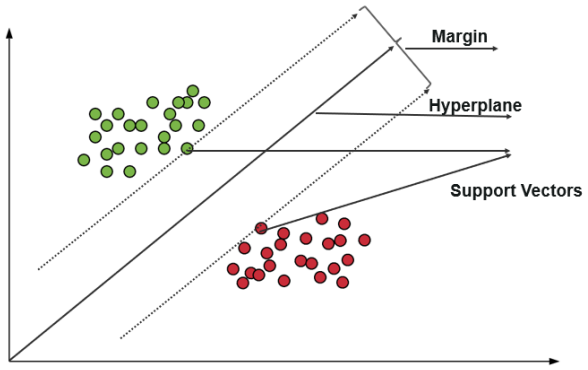


Figure 3.3: Example showing SVM classifier

*Chapter 4*

# Results and Discussion

## 4.1 Statistical Results - Liking Ratings

As mentioned in methods, we first examine differences in liking ratings specific to gender and musical expertise. To this end, we perform a non-parametric alternative to a two-way ANOVA called the permuted Wald-type statistic (WTP)[55], on the liking ratings wherein one factor represents gender while the other represents musical expertise. WTP was used because the liking ratings violated parametric ANOVA's normality and homogeneity of variance assumptions. WTP analysis revealed a significant main effect of musical expertise across all three stimuli (QN=5.877 for stimulus 1, QN=4.89 for stimulus 2, QN=5.699 for stimulus 3, all $p < 0.05$), Figure 4.1. As shown in Figure 4.1a, a significant effect of gender (QN=10.622, p=0.0026) is observed, and a borderline interaction (QN=3.813, p=0.059) with musical expertise for Stimulus 1. No significant effect of gender or interaction between gender and musical expertise is found in Stimulus 2 and 3.

## 4.2 Similarity Analysis

### 4.2.1 Similarities between different stimuli

The similarity coefficient was calculated between all possible stimulus pairs(S1 vs. S2, S2 vs. S3, and S1 vs. S3) for each subject to observe similarities between different stimuli. These values were then averaged across all subjects and different groups(18 musicians, 18 non-musicians, 17 males, and 19 females.

Overall, the results were highly similar between the different threshold methods. We report results for one standard deviation higher and lower than the overall mean value. As can be seen in Table 4.1, the spectral measure, Coherence, captures maximum variation, as evidenced by the low Sørensen-Dice coefficient. In contrast, the temporal measures show more significant overlap. Additionally, it was noted that IPS followed Coherence and then Wavelet Coherence regarding the level of similarity observed across different threshold methods. The results are similar across different groups of musicians, non-

musicians, males, and females. It can also be observed that the similarity is slightly high for non-musicians when compared to musicians. This may be due to non-musicians having more significant variability than musicians since musicians are trained in a specific instrument or genre of music, while non-musicians have more passive listening.

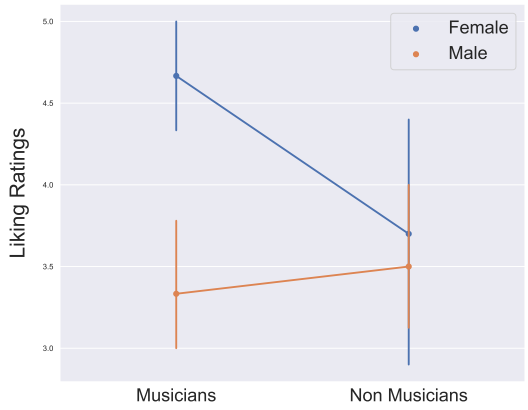


(a) Stimulus 1

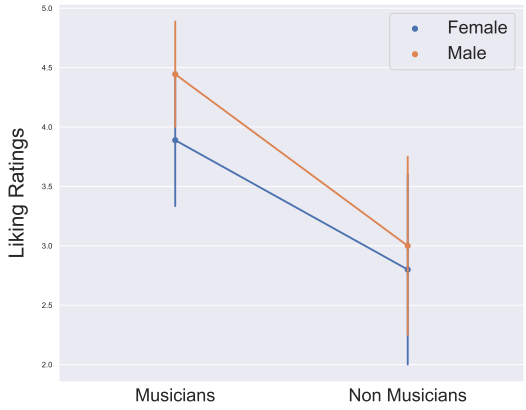


(b) Stimulus 2

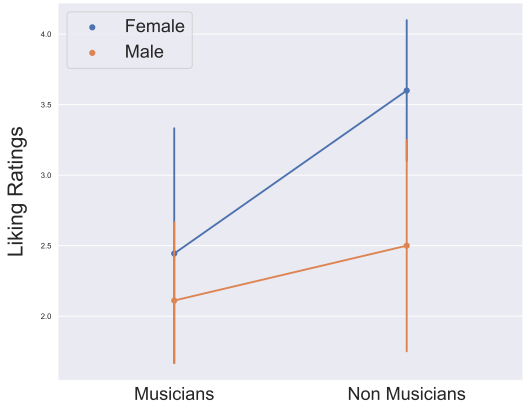


(c) Stimulus 3

Figure 4.1: Point plots for liking ratings grouped by musical expertise and gender.

### 4.2.2 Similarities between different groups

The similarity coefficient was calculated for each stimulus between all possible subject pairs(17 males x 19 females and 18 musicians x 18 non-musicians) to observe similarities between different groups. The mean value across all pairs for each stimulus was then calculated to compare different groups.

| FC Measure | All Subjects | | | Musicians | | | NonMusicians | | |
|---|---|---|---|---|---|---|---|---|---|
| | S1 vs S2 | S2 vs S3 | S1 vs S3 | S1 vs S2 | S2 vs S3 | S1 vs S3 | S1 vs S2 | S2 vs S3 | S1 vs S3 |
| **Cityblock Distance** | 0.6311 | 0.6427 | 0.6305 | 0.6221 | 0.6459 | 0.6087 | 0.6400 | 0.6394 | 0.6522 |
| **Coherence** | 0.3936 | 0.3927 | 0.3948 | 0.3934 | 0.3945 | 0.3923 | 0.3938 | 0.3909 | 0.3973 |
| **Cross Correlation** | 0.5262 | 0.5136 | 0.5055 | 0.5275 | 0.5198 | 0.4972 | 0.5250 | 0.5074 | 0.5138 |
| **DTW** | 0.6066 | 0.6191 | 0.6001 | 0.5952 | 0.6115 | 0.5707 | 0.6179 | 0.6266 | 0.6295 |
| **EMD** | 0.6016 | 0.6182 | 0.6033 | 0.5958 | 0.6236 | 0.5808 | 0.6074 | 0.6127 | 0.6259 |
| **Euclidean Distance** | 0.6353 | 0.6489 | 0.6353 | 0.6279 | 0.6522 | 0.6144 | 0.6428 | 0.6456 | 0.6562 |
| **IPS** | 0.4624 | 0.4650 | 0.4614 | 0.4537 | 0.4606 | 0.4542 | 0.4711 | 0.4695 | 0.4687 |
| **Mutual Information** | 0.4679 | 0.4652 | 0.4723 | 0.4639 | 0.4699 | 0.4546 | 0.4718 | 0.4605 | 0.4900 |
| **Pearson Correlation** | 0.4947 | 0.5009 | 0.5030 | 0.4913 | 0.5054 | 0.4856 | 0.4981 | 0.4964 | 0.5204 |
| **Spearman Correlation** | 0.4898 | 0.4908 | 0.4940 | 0.4840 | 0.4919 | 0.4763 | 0.4956 | 0.4896 | 0.5117 |
| **Wavelet Coherence** | 0.4133 | 0.4089 | 0.4124 | 0.4192 | 0.4198 | 0.4070 | 0.4074 | 0.3980 | 0.4179 |

(a) All Subjects, Musicians and NonMusicians

| FC Measure | Males | | | Females | | |
|---|---|---|---|---|---|---|
| | S1 vs S2 | S2 vs S3 | S1 vs S3 | S1 vs S2 | S2 vs S3 | S1 vs S3 |
| **Cityblock Distance** | 0.6169 | 0.6461 | 0.6245 | 0.6437 | 0.6395 | 0.6358 |
| **Coherence** | 0.3905 | 0.3858 | 0.3924 | 0.3964 | 0.3989 | 0.3970 |
| **Cross Correlation** | 0.5091 | 0.4899 | 0.4845 | 0.5416 | 0.5348 | 0.5243 |
| **DTW** | 0.5926 | 0.6230 | 0.5985 | 0.6190 | 0.6155 | 0.6016 |
| **EMD** | 0.5845 | 0.6225 | 0.5974 | 0.6169 | 0.6143 | 0.6086 |
| **Euclidean Distance** | 0.6199 | 0.6532 | 0.6283 | 0.6491 | 0.6451 | 0.6416 |
| **IPS** | 0.4648 | 0.4673 | 0.4647 | 0.4602 | 0.4630 | 0.4585 |
| **Mutual Information** | 0.4434 | 0.4429 | 0.4479 | 0.4898 | 0.4851 | 0.4941 |
| **Pearson Correlation** | 0.4746 | 0.4851 | 0.4916 | 0.5127 | 0.5150 | 0.5132 |
| **Spearman Correlation** | 0.4681 | 0.4735 | 0.4815 | 0.5092 | 0.5062 | 0.5052 |
| **Wavelet Coherence** | 0.4025 | 0.4062 | 0.4094 | 0.4229 | 0.4113 | 0.4152 |

(b) Males and Females

Table 4.1: Similarities measured by Sørensen-Dice similarity coefficient between different stimuli.

| FC Measure | Musicians vs Non-Musicians | | | Males vs Females | | |
|---|---|---|---|---|---|---|
| | Piazolla (S1) | DreamTheater (S2) | Rite of Spring (S3) | Piazolla (S1) | DreamTheater (S2) | Rite of Spring (S3) |
| **Cityblock Distance** | 0.8050 | 0.8136 | 0.7632 | 0.8026 | 0.7774 | 0.7795 |
| **Coherence** | 0.5962 | 0.5867 | 0.5715 | 0.5914 | 0.5884 | 0.5734 |
| **Cross Correlation** | 0.8172 | 0.7875 | 0.7507 | 0.7710 | 0.7071 | 0.7506 |
| **DTW** | 0.7559 | 0.7906 | 0.7132 | 0.7412 | 0.7014 | 0.7014 |
| **EMD** | 0.8005 | 0.8006 | 0.7599 | 0.7992 | 0.7691 | 0.7715 |
| **Euclidean Distance** | 0.8081 | 0.8121 | 0.7648 | 0.8074 | 0.7698 | 0.7858 |
| **IPS** | 0.7340 | 0.7322 | 0.7028 | 0.7114 | 0.7173 | 0.7193 |
| **Mutual Information** | 0.8040 | 0.7504 | 0.7609 | 0.7911 | 0.7476 | 0.7690 |
| **Pearson Correlation** | 0.7333 | 0.7155 | 0.7226 | 0.6892 | 0.7266 | 0.7350 |
| **Spearman Correlation** | 0.7309 | 0.7148 | 0.7175 | 0.6920 | 0.7283 | 0.7302 |
| **Wavelet Coherence** | 0.6915 | 0.6617 | 0.6519 | 0.6721 | 0.6714 | 0.6802 |

Table 4.2: Similarities measured by Sørensen-Dice similarity coefficient between different groups.

We can observe similar results from Table 4.2. Coherence is the least similarity-capturing measure, followed by Wavelet Coherence.

### 4.2.3 Similarities between different FC Measures

A group-level mean FC matrix was generated by averaging across all stimuli and subjects to observe similarities between different FC measures. A single mean FC matrix was obtained for each measure, which was subsequently thresholded to obtain binary adjacency matrices. The similarity coefficient was calculated between all possible FC measure pairs.

Figure 4.2 shows a high similarity between Cityblock Distance, Earth Mover's Distance (EMD), and Euclidean Distance. They all are dissimilarity measures and calculate distances between two points, with EMD being an exception since it represents the minimum cost of converting one distribution into the other. There is a high similarity between Pearson's and Spearman's Correlation. In addition, the spectral measure, Coherence, demonstrates high similarity with these two most commonly used temporal measures of FC.

## 4.3 Classification Results

Figure 4.3 shows the classification results. As can be seen, Pearson's correlation does not always stand out while differentiating the musicians from the non-musicians or males from females. Comparing performances of other measures, no one single FC measure particularly performed consistently better than the rest. Importantly, when we concatenate all these measures of FC, the composite measure almost always performs better. This could be due to thpoe contribution of other FC measures which potentially augment the discriminatory power of Pearson's correlation.

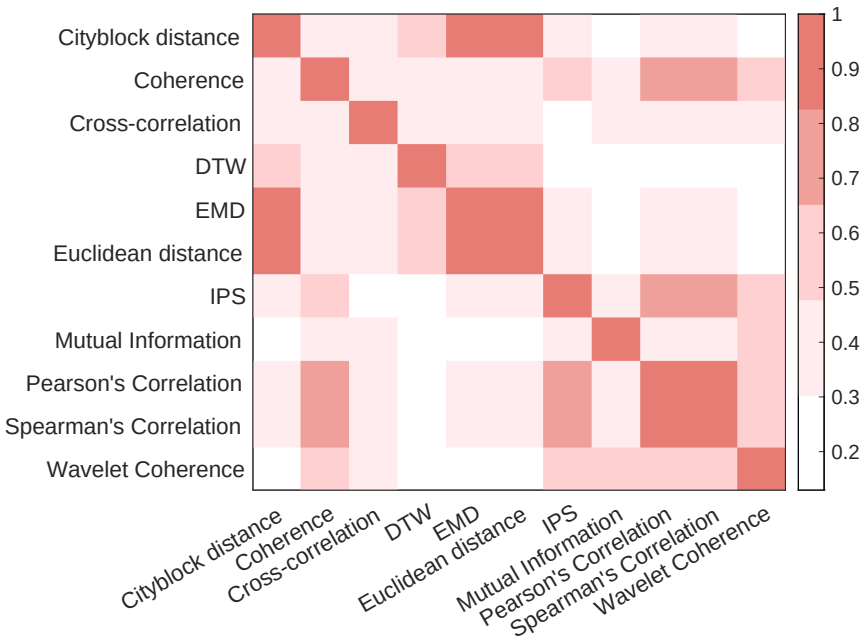


Figure 4.2: Similarities measured by Sørensen-Dice similarity coefficient between FC measures averaged across all stimulus and subjects.

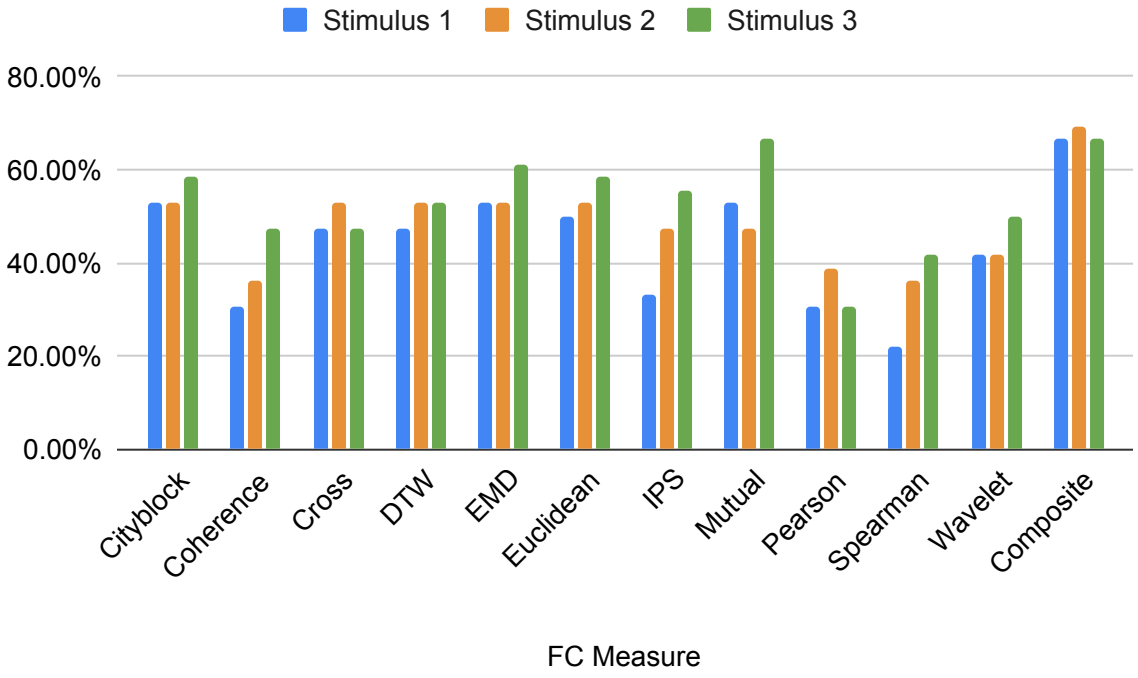


(a) Classification based on Musical Expertise

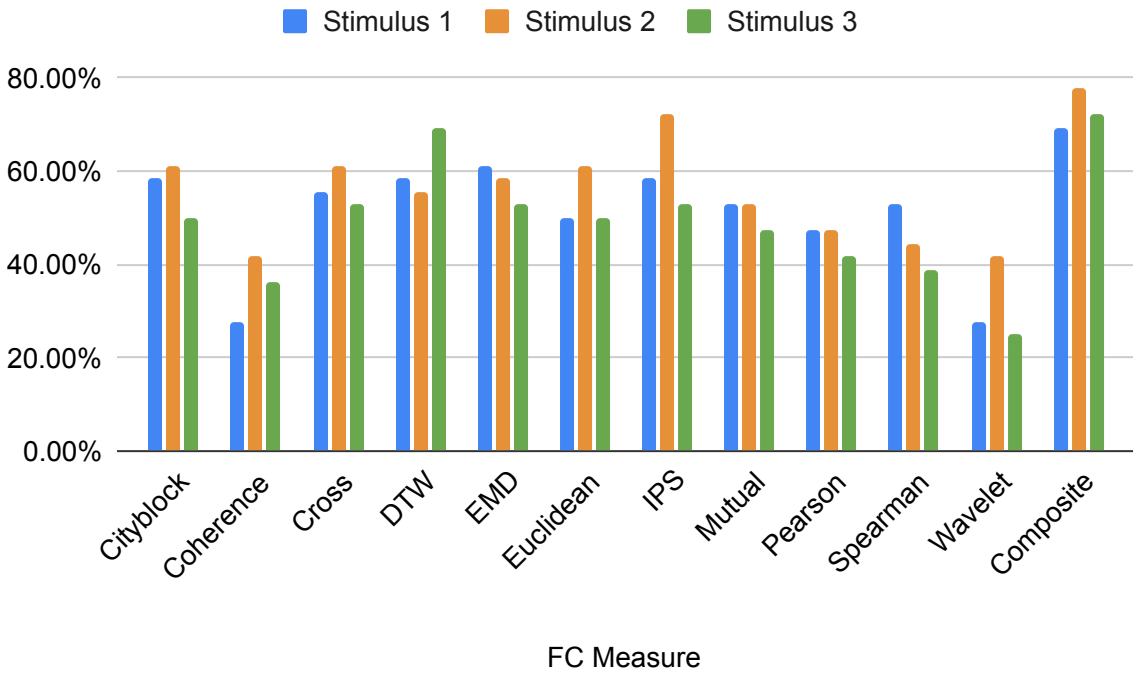


(b) Classification based on Gender

Figure 4.3: Classification accuracy for all three stimuli and FC measures.

*Chapter 5*

# Conclusions

Our study has made notable strides in understanding the relationship between musical preferences, gender, and musical expertise. The results align with previous research, indicating that musical preferences are indeed a personality trait. This was observed in the differences in liking ratings specific to gender and musical expertise. Females were found to prefer the tango and modern classical pieces over males, while males preferred the progressive rock piece. This is consistent with previous studies that found that females prefer more "mellow" musical styles with negative emotions and greater emotional depth, while males tend to prefer "harder" or "intense" styles.

The spectral measure, Coherence, consistently exhibited the least similarity and showed the highest variation across stimuli and groups compared to the temporal measures. This implies that different measures capture distinct information that may vary depending on the task or activity being performed and how they capture brain responses. This discovery holds particular importance as it offers a fresh perspective on utilizing diverse measures to capture a range of information effectively.

The comparison of all functional connectivity (FC) measures in classifying individuals based on gender and musical expertise aligns with the findings of Mohanty et al. (2020). There was no single FC measure that consistently outperformed others. However, a composite measure - a combination of all measures obtained by concatenation followed by a feature selection procedure was relatively more consistent and, in most cases, performed better than the rest of the measures. The study suggests that for analyses at a group level, temporal measures provide a more reliable and robust characterization of the FC patterns. These measures can be used in further studies to minimize the impact of individual variations and highlight the significant features that define the group.

The study achieved comparable results to the non-FC-based approach on the same dataset in Saari et al. (2018), which reported a classification accuracy of 77%. Using functional connectome during continuous music listening to classify gender and musical expertise is a novel approach as it leverages the functional connectivity measures to capture different statistical dependencies between two BOLD signals, including linear and non-linear dependencies.

However, the study acknowledges a few limitations. One such limitation is that the research was conducted using a relatively small dataset of 36 participants, which may have contributed to the low

accuracy results observed in the binary SVM-based classification. This constraint suggests that future studies could significantly benefit from larger sample sizes to enhance the accuracy of classification and increase the generalizability of the findings. Moreover, the observed low accuracy could be attributed to the features used in the analysis not being representative enough to adequately capture the individual differences. Additionally, the choice of the classifier used (SVM-based classification) may also have influenced the outcomes. Future investigations could explore alternative feature representations and classifiers to further refine the identification of individual differences based on brain responses to music.

The study used several functional connectivity (FC) measures, revealing novel insights. However, it suggests that future research could benefit from combining spectral and temporal measures to obtain a more comprehensive understanding of the underlying functional connectivity. This combination may provide a more complete picture of functional connectivity dynamics.

The research can be expanded in the future to investigate which regions contribute to classification. This would shed light on the essential functional connections related to musical expertise and gender. Understanding these connections could provide more detailed insights into how these factors influence musical preferences.

The study's findings are explained in the context of earlier research, and the results have been published in related publications. This study has not only contributed to the existing body of knowledge but also opened up new avenues for future research. The insights gained from this study are expected to have significant implications for the understanding of the relationship between music, gender, and musical expertise.

# Related Publications

- Predicting Individual Differences From Brain Responses to Music: A Comparison of Functional Connectivity Measures. Arihant Jain, Petri Toiviainen, Vinoo Alluri. **The 16th International Conference on Brain Informatics (BI) 2023, Hoboken & New Jersey, USA**.

  https://doi.org/10.1007/978-3-031-43075-6_17

- Predicting Individual Differences from Brain Responses to Music using Functional Network Centrality. Arihant Jain, Elvira Brattico, Petri Toiviainen, Vinoo Alluri. **2022 Conference on Cognitive Computational Neuroscience (CCN), San Fransisco, USA.**

  https://doi.org/10.32470/CCN.2022.1233-0

# Bibliography


[1] J. R. Hollenbeck and A. P. Brief, "The effects of individual differences and goal origin on goal setting and performance," *Organizational Behavior and Human Decision Processes*, vol. 40, no. 3, pp. 392–414, dec 1987. [Online]. Available: https://doi.org/10.1016%2F0749-5978%2887%2990023-9

[2] C. Gratton, T. O. Laumann, A. N. Nielsen, D. J. Greene, E. M. Gordon, A. W. Gilmore, S. M. Nelson, R. S. Coalson, A. Z. Snyder, B. L. Schlaggar, N. U. Dosenbach, and S. E. Petersen, "Functional brain networks are dominated by stable group and individual factors, not cognitive or daily variation," *Neuron*, vol. 98, no. 2, pp. 439–452.e5, Apr. 2018.

[3] D. M. Greenberg, S. Baron-Cohen, D. J. Stillwell, M. Kosinski, and P. J. Rentfrow, "Musical preferences are linked to cognitive styles," *PLOS ONE*, vol. 10, no. 7, p. e0131151, July 2015.

[4] A. Bonneville-Roussy, P. J. Rentfrow, M. K. Xu, and J. Potter, "Music through the ages: Trends in musical engagement and preferences from adolescence through middle adulthood." *Journal of Personality and Social Psychology*, vol. 105, no. 4, pp. 703–717, Oct. 2013.

[5] A. C. North, "Individual differences in musical taste," *The American Journal of Psychology*, vol. 123, no. 2, pp. 199–208, July 2010.

[6] P. J. Rentfrow and S. D. Gosling, "The do re mi's of everyday life: The structure and personality correlates of music preferences." *Journal of Personality and Social Psychology*, vol. 84, no. 6, pp. 1236–1256, 2003.

[7] V. Alluri, P. Toiviainen, I. Burunat, M. Kliuchko, P. Vuust, and E. Brattico, "Connectivity patterns during music listening: Evidence for action-based processing in musicians," *Human Brain Mapping*, vol. 38, no. 6, pp. 2955–2970, Mar. 2017.

[8] R. C. Gur, B. I. Turetsky, M. Matsui, M. Yan, W. Bilker, P. Hughett, and R. E. Gur, "Sex differences in brain gray and white matter in healthy young adults: Correlations with cognitive performance," *The Journal of Neuroscience*, vol. 19, no. 10, pp. 4065–4072, May 1999. [Online]. Available: https://doi.org/10.1523/jneurosci.19-10-04065.1999

[9] M. Hines, "Gender development and the human brain," *Annual Review of Neuroscience*, vol. 34, no. 1, pp. 69–88, jul 2011. [Online]. Available: https://doi.org/10.1146%2Fannurev-neuro-061010-113654

[10] L. Cahill, "Why sex matters for neuroscience," *Nature Reviews Neuroscience*, vol. 7, no. 6, pp. 477–484, May 2006. [Online]. Available: https://doi.org/10.1038/nrn1909

[11] L. Cahill, M. Uncapher, L. Kilpatrick, M. T. Alkire, and J. Turner, "Sex-related hemispheric lateralization of amygdala function in emotionally influenced memory: An fMRI investigation," *Learning &amp Memory*, vol. 11, no. 3, pp. 261–266, may 2004. [Online]. Available: https://doi.org/10.1101%2Flm.70504

[12] M. Ingalhalikar, A. Smith, D. Parker, T. D. Satterthwaite, M. A. Elliott, K. Ruparel, H. Hakonarson, R. E. Gur, R. C. Gur, and R. Verma, "Sex differences in the structural connectome of the human brain," *Proceedings of the National Academy of Sciences*, vol. 111, no. 2, pp. 823–828, Dec. 2013.

[13] S. Koelsch, B. Maess, T. Grossmann, and A. D. Friederici, "Electric brain responses reveal gender differences in music processing," *NeuroReport*, vol. 14, no. 5, pp. 709–713, apr 2003. [Online]. Available: https://doi.org/10.1097%2F00001756-200304150-00010

[14] A. C. North, D. J. Hargreaves, and S. A. O'Neill, "The importance of music to adolescents," *British Journal of Educational Psychology*, vol. 70, no. 2, pp. 255–272, June 2000.

[15] A. Angulo-Perkins, W. Aubé, I. Peretz, F. A. Barrios, J. L. Armony, and L. Concha, "Music listening engages specific cortical regions within the temporal lobes: Differences between musicians and non-musicians," *Cortex*, vol. 59, pp. 126–137, Oct. 2014.

[16] C. Gaser and G. Schlaug, "Brain structures differ between musicians and non-musicians," *The Journal of Neuroscience*, vol. 23, no. 27, pp. 9240–9245, Oct. 2003.

[17] ——, "Brain structures differ between musicians and non-musicians," *The Journal of Neuroscience*, vol. 23, no. 27, pp. 9240–9245, oct 2003. [Online]. Available: https://doi.org/10.1523%2Fjneurosci.23-27-09240.2003

[18] A. Imfeld, M. S. Oechslin, M. Meyer, T. Loenneker, and L. Jancke, "White matter plasticity in the corticospinal tract of musicians: A diffusion tensor imaging study," *NeuroImage*, vol. 46, no. 3, pp. 600–607, July 2009.

[19] S. Hutchinson, "Cerebellar volume of musicians," *Cerebral Cortex*, vol. 13, no. 9, pp. 943–949, sep 2003. [Online]. Available: https://doi.org/10.1093%2Fcercor%2F13.9.943

[20] V. Alluri, E. Brattico, P. Toiviainen, I. Burunat, B. Bogert, J. Numminen, and M. Kliuchko, "Musical expertise modulates functional connectivity of limbic regions during continuous music listening." *Psychomusicology: Music, Mind, and Brain*, vol. 25, no. 4, pp. 443–454, Dec. 2015.

[21] D. Niranjan, P. Toiviainen, E. Brattico, and V. Alluri, "Dynamic functional connectivity in the musical brain," in *Brain Informatics*. Springer International Publishing, 2019, pp. 82–91.

[22] S. Koelsch, E. Schröger, and M. Tervaniemi, "Superior pre-attentive auditory processing in musicians," *Neuroreport*, vol. 10, no. 6, pp. 1309–1313, 1999.

[23] S. Ogawa, T. M. Lee, A. R. Kay, and D. W. Tank, "Brain magnetic resonance imaging with contrast dependent on blood oxygenation." *Proceedings of the National Academy of Sciences*, vol. 87, no. 24, pp. 9868–9872, Dec. 1990. [Online]. Available: https://doi.org/10.1073/pnas.87.24.9868

[24] S. Huettel, A. Song, and G. McCarthy, *Functional Magnetic Resonance Imaging*. Oxford University Press, Incorporated, 2009. [Online]. Available: https://books.google.co.in/books?id=BNhMPgAACAAJ

[25] B. Biswal, F. Z. Yetkin, V. M. Haughton, and J. S. Hyde, "Functional connectivity in the motor cortex of resting human brain using echo-planar mri," *Magnetic Resonance in Medicine*, vol. 34, no. 4, pp. 537–541, Oct. 1995. [Online]. Available: https://doi.org/10.1002/mrm.1910340409

[26] M. P. van den Heuvel and H. E. H. Pol, "Exploring the brain network: A review on resting-state fMRI functional connectivity," *European Neuropsychopharmacology*, vol. 20, no. 8, pp. 519–534, Aug. 2010. [Online]. Available: https://doi.org/10.1016/j.euroneuro.2010.03.008

[27] B. Rashid, E. Damaraju, G. D. Pearlson, and V. D. Calhoun, "Dynamic connectivity states estimated from resting fMRI identify differences among schizophrenia, bipolar disorder, and healthy control subjects," *Frontiers in Human Neuroscience*, vol. 8, nov 2014. [Online]. Available: https://doi.org/10.3389%2Ffnhum.2014.00897

[28] B. Rashid, M. R. Arbabshirani, E. Damaraju, M. S. Cetin, R. Miller, G. D. Pearlson, and V. D. Calhoun, "Classification of schizophrenia and bipolar patients using static and dynamic resting-state fMRI brain connectivity," *NeuroImage*, vol. 134, pp. 645–657, July 2016. [Online]. Available: https://doi.org/10.1016/j.neuroimage.2016.04.051

[29] U. Hasson and C. J. Honey, "Future trends in neuroimaging: Neural processes as expressed within real-life contexts," *NeuroImage*, vol. 62, no. 2, pp. 1272–1278, Aug. 2012. [Online]. Available: https://doi.org/10.1016/j.neuroimage.2012.02.004

[30] J. Zaki and K. Ochsner, "The need for a cognitive neuroscience of naturalistic social cognition," *Annals of the New York Academy of Sciences*, vol. 1167, no. 1, pp. 16–30, June 2009. [Online]. Available: https://doi.org/10.1111/j.1749-6632.2009.04601.x

[31] J. Zaki and K. N. Ochsner, "The neuroscience of empathy: progress, pitfalls and promise," *Nature Neuroscience*, vol. 15, no. 5, pp. 675–680, Apr. 2012. [Online]. Available: https://doi.org/10.1038/nn.3085

[32] U. Hasson, Y. Nir, I. Levy, G. Fuhrmann, and R. Malach, "Intersubject synchronization of cortical activity during natural vision," *Science*, vol. 303, no. 5664, pp. 1634–1640, Mar. 2004. [Online]. Available: https://doi.org/10.1126/science.1089506

[33] K. J. Friston, *Brain Connectivity*, vol. 1, no. 1, pp. 13–36, jan 2011. [Online]. Available: https://doi.org/10.1089%2Fbrain.2011.0008

[34] M. P. van den Heuvel and H. E. H. Pol, "Exploring the brain network: A review on resting-state fMRI functional connectivity," *European Neuropsychopharmacology*, vol. 20, no. 8, pp. 519–534, aug 2010. [Online]. Available: https://doi.org/10.1016%2Fj.euroneuro.2010.03.008

[35] J. S. Damoiseaux, S. A. R. B. Rombouts, F. Barkhof, P. Scheltens, C. J. Stam, S. M. Smith, and C. F. Beckmann, "Consistent resting-state networks across healthy subjects," *Proceedings of the National Academy of Sciences*, vol. 103, no. 37, pp. 13 848–13 853, Sept. 2006.

[36] M. D. Greicius, B. Krasnow, A. L. Reiss, and V. Menon, "Functional connectivity in the resting brain: A network analysis of the default mode hypothesis," *Proceedings of the National Academy of Sciences*, vol. 100, no. 1, pp. 253–258, Dec. 2002.

[37] W. R. Shirer, S. Ryali, E. Rykhlevskaia, V. Menon, and M. D. Greicius, "Decoding subject-driven cognitive states with whole-brain connectivity patterns," *Cerebral Cortex*, vol. 22, no. 1, pp. 158–165, May 2011.

[38] I. Burunat, E. Brattico, T. Puoliväli, T. Ristaniemi, M. Sams, and P. Toiviainen, "Action in perception: Prominent visuo-motor functional symmetry in musicians during music listening," *PLOS ONE*, vol. 10, no. 9, p. e0138238, Sept. 2015.

[39] I. Burunat, V. Tsatsishvili, E. Brattico, and P. Toiviainen, "Coupling of action-perception brain networks during musical pulse processing: Evidence from region-of-interest-based independent component analysis," *Frontiers in Human Neuroscience*, vol. 11, May 2017. [Online]. Available: https://doi.org/10.3389/fnhum.2017.00230

[40] P. Saari, I. Burunat, E. Brattico, and P. Toiviainen, "Decoding musical training from dynamic processing of musical features in the brain," *Scientific Reports*, vol. 8, no. 1, Jan. 2018.

[41] R. Sladky, K. J. Friston, J. Tröstl, R. Cunnington, E. Moser, and C. Windischberger, "Slice-timing effects and their correction in functional MRI," *NeuroImage*, vol. 58, no. 2, pp. 588–594, Sept. 2011. [Online]. Available: https://doi.org/10.1016/j.neuroimage.2011.06.078

[42] D. L. Collins, P. Neelin, T. M. Peters, and A. C. Evans, "Automatic 3D intersubject registration of MR volumetric data in standardized talairach space," *J. Comput. Assist. Tomogr.*, vol. 18, no. 2, pp. 192–205, Mar. 1994.

[43] S. Arslan, S. I. Ktena, A. Makropoulos, E. C. Robinson, D. Rueckert, and S. Parisot, "Human brain mapping: A systematic comparison of parcellation methods for the human cerebral cortex," *NeuroImage*, vol. 170, pp. 5–30, Apr. 2018. [Online]. Available: https://doi.org/10.1016/j.neuroimage.2017.04.014

[44] R. C. Craddock, G. James, P. E. Holtzheimer, X. P. Hu, and H. S. Mayberg, "A whole brain fMRI atlas generated via spatially constrained spectral clustering," *Human Brain Mapping*, vol. 33, no. 8, pp. 1914–1928, July 2011. [Online]. Available: https://doi.org/10.1002/hbm.21333

[45] A. Altmann, B. Ng, S. M. Landau, W. J. Jagust, and M. D. Greicius, "Regional brain hypometabolism is unrelated to regional amyloid plaque burden," *Brain*, vol. 138, no. 12, pp. 3734–3746, Sept. 2015. [Online]. Available: https://doi.org/10.1093/brain/awv278

[46] T. Sørensen, T. Sørensen, T. Biering-Sørensen, T. Sørensen, and J. T. Sorensen, "A method of establishing group of equal amplitude in plant sociobiology based on similarity of species content and its application to analyses of the vegetation on danish commons," 1948.

[47] L. R. Dice, "Measures of the amount of ecologic association between species," *Ecology*, vol. 26, no. 3, pp. 297–302, July 1945.

[48] R. Mohanty, W. A. Sethares, V. A. Nair, and V. Prabhakaran, "Rethinking measures of functional connectivity via feature extraction," *Scientific Reports*, vol. 10, no. 1, Jan. 2020.

[49] S. L. Simpson, F. D. Bowman, and P. J. Laurienti, "Analyzing complex functional brain networks: Fusing statistics and network science to understand the brain," *Statistics Surveys*, vol. 7, no. none, Jan. 2013.

[50] Q. K. Telesford, S. L. Simpson, J. H. Burdette, S. Hayasaka, and P. J. Laurienti, "The brain as a complex system: Using network science as a tool for understanding the brain," *Brain Connectivity*, vol. 1, no. 4, pp. 295–308, Oct. 2011.

[51] P. J. Laurienti, K. E. Joyce, Q. K. Telesford, J. H. Burdette, and S. Hayasaka, "Universal fractal scaling of self-organized networks," *Physica A: Statistical Mechanics and its Applications*, vol. 390, no. 20, pp. 3608–3613, Oct. 2011.

[52] L. Breiman, *Machine Learning*, vol. 45, no. 1, pp. 5–32, 2001.

[53] P. Geurts, D. Ernst, and L. Wehenkel, "Extremely randomized trees," *Machine Learning*, vol. 63, no. 1, pp. 3–42, Mar. 2006.

[54] F. Pedregosa, G. Varoquaux, A. Gramfort, V. Michel, B. Thirion, O. Grisel, M. Blondel, P. Prettenhofer, R. Weiss, V. Dubourg, J. Vanderplas, A. Passos, D. Cournapeau, M. Brucher, M. Perrot, and E. Duchesnay, "Scikit-learn: Machine learning in Python," *Journal of Machine Learning Research*, vol. 12, pp. 2825–2830, 2011.

[55] S. Friedrich, E. Brunner, and M. Pauly, "Permuting longitudinal data in spite of the dependencies," *Journal of Multivariate Analysis*, vol. 153, pp. 255–265, Jan. 2017.